Section 9

Development of and studies with coupled ocean-atmosphere models

Analysis of Inferred Cyclogenesis Frequency in ERA-40 Reanalysis and in an Ensemble of Models

Louis-Philippe Caron[1] Colin G. Jones[1]
[1] *Université du Québec à Montréal, CRCMD Network*
emails: lpcaron@sca.uqam.ca, jones.colin@uqam.ca

Introduction

Predictions regarding future tropical cyclone (TC) activity would ideally be done using a Coupled Global Climate Models (CGCMs) capable of resolving TCs, where TCs statistics in two different simulations, one using present-day level of greenhouse gases and one using projected level of greenhouse gases, would be compared. However, due to their coarse resolution, CGCMs are unable to resolve TCs. Hence, the results of studies based on what has been coined Tropical Cyclone-Like Vortices (TCLVs)) remain inconclusive since they are not based on realistic TCs. To circumvent this problem, a different approach can be used where the frequency of TCs is inferred from the temporal evolution of the main large-scale climatic fields we believe to control their frequency of occurence and distribution.

Methodology

To infer seasonal TCs frequency, Gray (1975) proposed the use of an index, the Seasonal Genesis Parameter (SGP), which was found to be a good predictor of the number of TCs formed in a three months period per 5° × 5° latitude-longitude square per 20 years. The SGP is the product of a dynamical potential and a thermal potential, each of which is based on the product of three factors, such that:

$$\text{SGP} = \underbrace{(|f| \times I_\zeta \times I_{WS})}_{\text{Dynamic potential}} \times \underbrace{(E \times I_\theta \times I_{RH})}_{\text{Thermal potential}}$$

where

- f is the Coriolis parameter at a given latitude.
- $I_\zeta = \zeta \frac{f}{|f|} + 5$ with ζ being the low level relative vorticity at 925 hPa.
- $I_{WS} = \left(\left|\frac{\delta V}{\delta P} + 3\right|\right)^{-1}$ is the inverse of the vertical wind shear of the horizontal wind (V) between pressure (P) levels 925 hPa and 200 hPa.
- $E = \int_0^{60} \rho_w c_w (T - 26)\, dz$ measures the thermal energy of the ocean between the surface and 60 m depth (ρ_w and c_w are density and specific heat capacity of sea water).
- $I_\theta = \left(\frac{\delta\theta}{\delta P} + 5\right)$ is the moist static stability defined as the vertical gradient of the equivalent potential temperature θ_e between the surface and 500 hPa.
- $I_{RH} = Max\left(\frac{RH-40}{30}, 1\right)$, where RH is the average relative humidity in percent between 500 hPa and 700 hPa.

These components summarize the main dynamical and thermodynamic large scale variables that are believed to determine whether the atmosphere-ocean system can support TC development. If any of the components of the SGP is less than or equal to zero, the SGP is set to zero. The SGP is usually divided between the winter (JFM), spring (AMJ), summer (JAS) and fall (OND). The Yearly Genesis Parameter (YGP) is calculated as the sum of the four SGPs. By comparion, the Convective SGP (CSGP) (Royer et. al., 1998), another index to estimate TC frequency, replaces the thermal potential of the SGP by a convective potential defined as

$$\text{convective potential} = k \times P_c \text{ over the oceans}$$

where P_C is the seasonal mean convective precipitation computed by a given model. The CSGPs can also be summed over all seasons to give a CYGP. The proportionality factor k was defined such that the total number of cyclones over the globe given by the CYGP be the same as the original YGP for the present climate using ERA-40 reanalysis.

In this study, we first validate the use of both indices by comparing the inferred number of TCs using ERA-40 reanalysis data for the period 1983-2002 to the actual number of TCs for the same period. We then analyze the YGP and CYGP in the present climate for an ensemble of six CGCMs and compare the quality of their predictions to both observations and ERA-40 reanalysis data.

Observations were taken from Joint Typhoon Warning Center (JTWC) best track data set for the Southern Hemisphere, West North Pacific and Northern Indian Ocean and from the National Hurricane Center (NHC) best track data set for the Atlantic and Eastern North Pacific. A storm was considered a tropical cyclone whenever the surface sustained winds reached 17 m/s.

Results

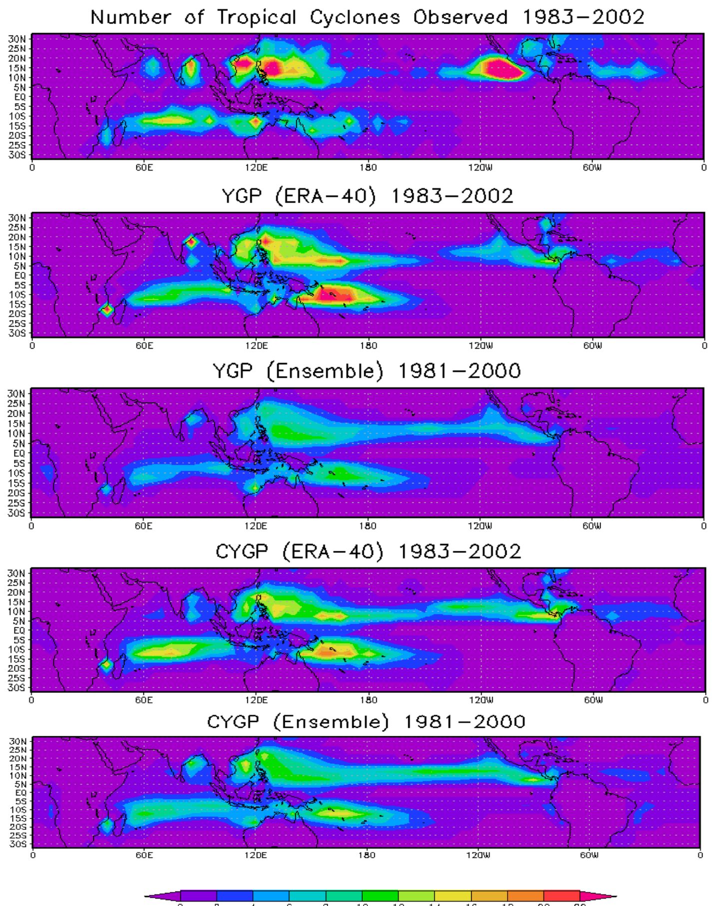

Figure 1: Tropical cyclone genesis per 20 years as given by a) observation and predicted by b) d) ERA-40 reanalysis data and c) e) an ensemble of IPCC models.

Figure 1 shows the YGP and CYGP calculated from ERA-40 reanalysis and the ensemble mean of 6 CGCMs simulations for the same nominal period. The YGP and CYGP as computed using the ERA-40 reanalysis data for the period 1983-2002 compare favorably to the actual number of tropical cyclones for the same period: the mean annual number of cyclones during that 20 years period was 86 while the number predicted by ERA-40 for YGP and CYGP is 83. However, the proportion of cyclones is too high in the Southern Hemisphere (SH) and too low in the Northern Hemisphere (NH). More specifically, TC genesis is underestimated in the NE Pacific and Atlantic while it is overestimated in the SW Pacific. Also, the YGP fails to predict TC activity in the Arabian Sea. By opposition, especially in the case of the CYGP, the genesis parameters predict the frequent formation of TCs in the Central Pacific where in fact few actually occur.

We then performed a similar analysis on an ensemble of six CGCMs (CGCM 3.1, ECHAM 5, GFDL-CM 2.0, GFDL-CM 2.1, MIROC 3.2 (hi-resolution) and HadGEM 1) whose simulations were submitted to the IPCC for the 4th assessment report. The analysis was done for the period 1981-2000 in the scenario of the 20th Century. In this case, the number of TCs is clearly underestimated by the YGP, which predicts an average of 58 $TCs/year$, while the CYGP, if using the same proportionality factor k as with ERA-40, predicts 85 $TCs/year$. There is a large variability between individual models, with respect to both YGP and CYGP: using the YGP, the predictions varied from 29 $TCs/year$ (CGCM 3.1) to 121 $TCs/year$ (ECHAM 5) while the CYGP varied from 48 $TCs/year$ (MIROC 3.2) to 120 $TCs/year$ (ECHAM 5). Again, the geographical distribution of predicted TCs shows some discrepancies. Most noticeable is the almost complete absence of TC formation in the Atlantic. This was caused by the vorticity factor which is found to be 0 over large portion of that basin. Similarly to ERA-40, the models also underestimate TC genesis in the NE Pacific and in the Arabian Sea and predict frequent TC formation in Central Pacific, contrary to observations. The CYGP also predict unrealistic TC activity off the coasts of South America in the SH.

Having validated the use of the parameters on both ERA-40 and an ensemble of CGCMs, future research will look at the time evolution of those same parameters to detect the possible emergence of a trend in the inferred TC statistics when CO_2 levels are increased in the models.

References:

Gray, W. (1975): Tropical Cyclone Genesis, Dept. of Atmospheric Science Paper, No. 234, Colorado State University, Fort Collins, CO, p. 121.

Royer, J.-F., F. Chauvin, B. Timbal, P. Araspin and D. Grimal (1998): A GCM Study of the Impact Greenhouse Gas Increase on the Frequency of Occurrence of Tropical Cyclones,*Climatic Change*, **38**, 307-343.

Coupled climate–methane cycle simulation with a climate model of intermediate complexity forced by SRES A2 scenario

A.V. Eliseev, I.I. Mokhov, M.M. Arzhanov,P.F. Demchenko, and S.N. Denisov

A.M. Obukhov Institute of Atmospheric Physics RAS,
3 Pyzhevsky, 1091017 Moscow, Russia, e–mail: eliseev@ifaran.ru

The climate model of intermediate complexity developed at the A.M. Obukhov Insitute of Atmospheric Physics RAS (IAP RAS CM) [6] is extended by modules of soil thaw/freeze cycles [2] and methane cycle. The latter is based on [7] with a prescribed characteristic time of chemical decompostion of methane in the atmosphere $\tau_{CH_4,atm} = 10.5\ yr$. Methane emissions from bogs and swamps are computed based on [1] but with some parameters tuned. Other non–anthropogenic methane sources are prescribed. A simulation with IAP RAS CM is performed which is forced by the anthropogenic emissions of CO_2 and CH_4 and atmospheric concentration of N_2O. These forcings are changed in accordance to the corresponding historical estimations extended back to 1610 for the 17th–20th centuries and in accordance to scenarios SRES A2 [3] for the 21st century. To match the historical and future methane emissions the former are uniformly reduced on 13%. One simulation (CPL) employs a fully coupled model. The other simulation (UCPL) forces the modules of soil thaw/freeze cycles and methane cycle by the monthly mean climatologies of surface air temperature and precipitation obtained from the control preindustrial simulation with IAP RAS CM.

Simulated methane emissions from bogs and swamps $E_{\mathrm{CH_4,bs}}$ amount about 130 $MtCH_4/yr$ before the mid 20th century (Fig. 1). They increase to $\approx 145\ MtCH_4/yr$ to the late 20th century. These values are in agreement with observational estimates $145 \pm 30\ MtCH_4/yr$ [4]. In the 21st century, methane emissions from wetlands increases drastically, up to $\approx 200\ MtCH_4/yr$. This increase is basically due to temperature dependence of apparent methane production.

Simulated concentration of methane in the atmosphere $p\mathrm{CH_{4,a}}$ is overestimated slightly before the middle of the 20th century. This is presumably due to neglection of other external forcings (solar irradiance, volcanos, aerosols) leading to too rapid and too early warming during the 20th century in IAP RAS CM [6] (as well as in other climate models [3]). An agreement improves in the second part of the 20th century. Rapid buildup of methane in the atmosphere due to anthropogenic emissions lead to $p\mathrm{CH_{4,a}} = 3904\ ppbv$ in the end of the 21st century in the simulation CPL. In the simulation UCPL, owing to lack of the enhancement of the methane emissions from wetlands, this value is smaller, 3671 $ppbv$.

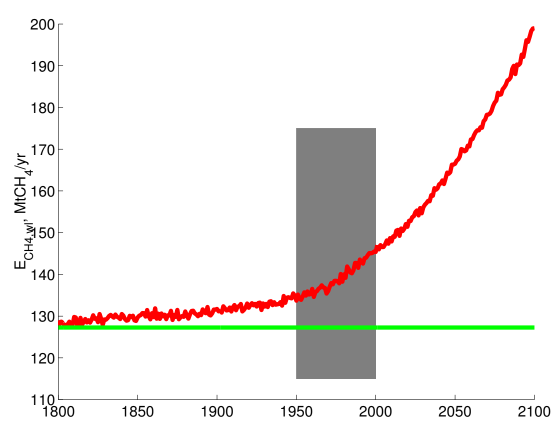

Figure 1: Modelled methane emissions from wetlands for the simulations CPL and UCPL (red and green lines, respectively) together with a corresponding observational range [4] (gray) .

l9cm

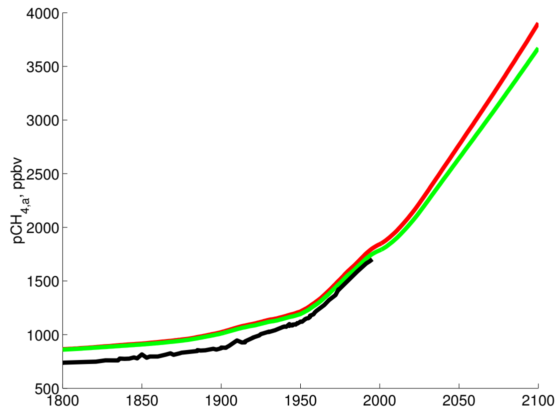

Figure 2: Modelled concentration of methane in the atmosphere for the simulations CPL and UCPL (red and green lines, respectively) together with a historical data [5] (black) .

Annual mean surface air temperature (SAT) in 2071–2100 in the simulation CPL is warmer (by $0.2 - 0.6\ K$) over the subtropical northern land in comparison to that obtained in the simulation UCPL. In contrast, SAT in CPL during the same period is lower over the northernmost land areas, Mideterranean, and North America midlatitudes by the same amount. When SAT is averaged globally, this anomalies are mutually compensated and global SAT for this period is almost indistinguishable between the simulations CPL and UCPL.

This work is supported by the Russian Foundation for Basic Research, by the programs of the Russian Academy of Sciences, and by the Russian President scientific grant.

References

[1] T.R. Christensen and P. Cox. Response of methane emission from arctic tundra to climatic change: results from a model simulation. *Tellus*, 47B(3):301–309, 1995.

[2] A.V. Eliseev, M.M. Arzhanov, P.F. Demchenko, S.N. Denisov, and I.I. Mokhov. Permafrost response to SRES A2 greenhouse forcing in a climate model of intermediate complexity. 2007. (this issue).

[3] J.T. Houghton, Y. Ding, D.J. Griggs, M. Noguer, P.J. van der Linden, X. Dai, K. Maskell, and C.A. Johnson, editors. *Climate Change 2001: The Scientific Basis. Contribution of Working Group I to the Third Assessment Report of the Intergovernmental Panel on Climate Change.* Cambridge University Press, Cambridge/New York, 2001.

[4] J. Lelieveld, P.J. Crutzen, and F.J. Dentener. Changing concentration, lifetime and climate forcing of atmospheric methane. *Tellus*, 50B(2):128–150, 1998.

[5] C. MacFarling Meure, D. Etheridge, C. Trudinger, P. Steele, R. Langenfelds, T. van Ommen, A. Smith, and J. Elkins. Law dome CO_2, CH_4 and N_2O ice core records extended to 2000 years BP. *Geophys. Res. Lett.*, 33(14):L14810, 2006.

[6] I.I. Mokhov, V.A. Bezverkhnii, A.V. Eliseev, and A.A. Karpenko. Model estimates of global climatic changes in the 21st century with account for different variation scenarios of solar activity. *Doklady Earth Sci.*, 411(8):1327–1330, 2006.

[7] T.J. Osborn and T.M.L. Wigley. A simple model for estimating methane concentration and lifetime variations. *Clim. Dyn.*, 9(4-5):181–193, 1994.

Permafrost response to SRES A2 greenhouse forcing in a climate model of intermediate complexity

A.V. Eliseev, M.M. Arzhanov,P.F. Demchenko,
S.N. Denisov, and I.I. Mokhov

A.M. Obukhov Institute of Atmospheric Physics RAS,
3 Pyzhevsky, 1091017 Moscow, Russia, e–mail: eliseev@ifaran.ru

The climate model of intermediate complexity developed at the A.M. Obukhov Insitute of Atmospheric Physics RAS (IAP RAS CM) [4] is extended by modules of soil thaw/freeze cycles [3] and methane cycle [1]. Two simulation with IAP RAS CM are performed which both are forced by the anthropogenic emissions of CO_2 and CH_4 and atmospheric concentration of N_2O. These forcings are changed in accordance to the corresponding historical estimations extended back to 1610 [4] for the 17th–20th centuries and in accordance to scenarios SRES A2 [2] for the 21st century.

The simulated area of the permafost extension changes little till the mid 20th century varying in the range $12.5 - 13.5$ $mln\ km^2$ (Fig. 1). This value is between the estimated areas of the continious (10.7 $mln\ km^2$) and total (22.8 $mln\ km^2$). permafrost extensions [5]. Geographical distribution of the simulated permafrost looks as a whole realistic if compared with the map from [5]. A notable exception is the region near the Baltic Sea where IAP RAS CM simulates permafrost absent in the observations. This bias as a reflection of the overall model's cold bias in the high latitude continents. In addition, permafrost over the Tibetian plato is not simulated owing to the lack of orography in the model.

In the model, permafrost cover shrinks rapidly in the late 20th–early 21st centuries. In the mid 21st century area of the permafrost extension attains the value 9.0 $mln\ km^2$ (Fig. 1) and changes little afterwards. Permafrost disappears in the most European regions but remains in Asia and North America. However, over the latter two continents, the annual thaw depth increases substantionally in the late 21st century compared to the earlier periods (Fig. 2).

This work is supported by the Russian Foundation for Basic Research, by the programs of the Russian Academy of Sciences, and by the Russian President scientific grant.

References

[1] A.V. Eliseev, M.M. Arzhanov, P.F. Demchenko, S.N. Denisov, and I.I. Mokhov. Coupled climate–methane cycle simulation with a climate model of intermediate complexity forced by SRES A2 scenario. 2007. (this issue).

[2] J.T. Houghton, Y. Ding, D.J. Griggs, M. Noguer, P.J. van der Linden, X. Dai, K. Maskell, and C.A. Johnson, editors. *Climate Change 2001: The Scientific Basis. Contribution of Working Group I to the Third Assessment Report of the Intergovernmental Panel on Climate Change.* Cambridge University Press, Cambridge/New York, 2001.

[3] V.A. Kudryavtsev, L.S. Garagula, K.A. Kondratiyeva, and V.E. Melamed. *Frost Forecasting in Geological Engineering Investigations,*. CRREL, Hanover, NH, 1977.

[4] I.I. Mokhov, V.A. Bezverkhnii, A.V. Eliseev, and A.A. Karpenko. Model estimates of global climatic changes in the 21st century with account for different variation scenarios of solar activity. *Doklady Earth Sci.*, 411(8):1327–1330, 2006.

[5] T. Zhang, R.G. Barry, K. Knowles, J.A. Heginbottom, and J. Brown. Statistics and characteristics of permafrost and ground–ice distribution in the Northern Hemisphere. *Polar Geogr.*, 23(2):132–154, 1999.

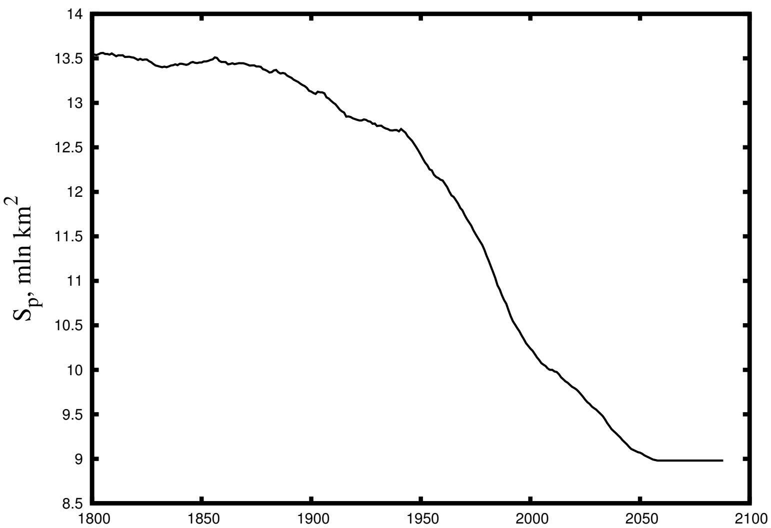

Figure 1: Area of the permafrost extension simulated by IAP RAS CM (a 25–yr moving average is applied).

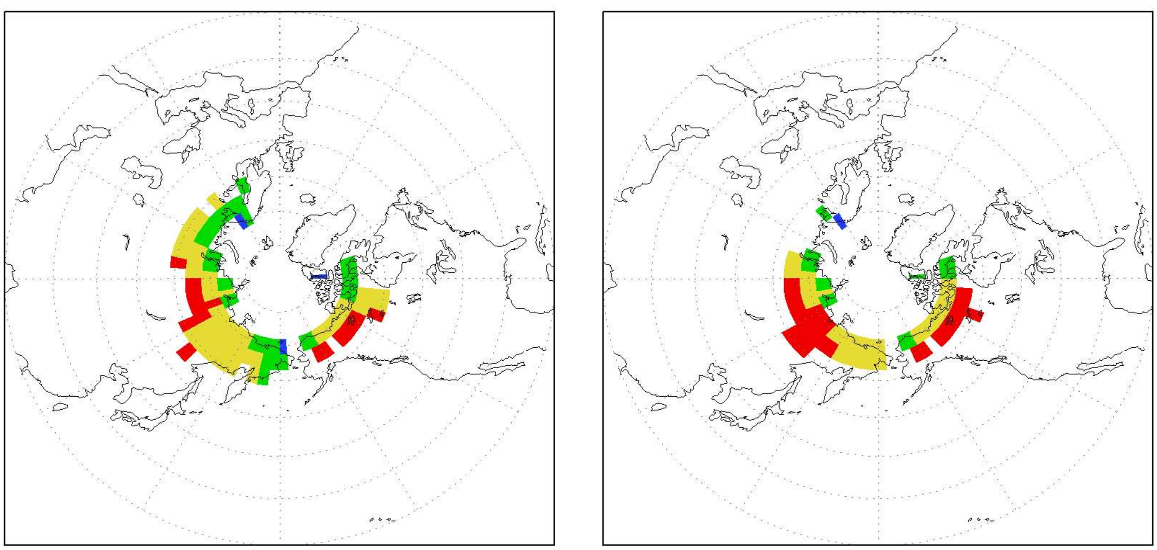

Figure 2: Mean seasonal thaw depth (in meters) simulated by IAP RAS CM for 1961–2000 and 2071–2100 (left and right panels respectively). The colour figures ranges of thaw depth $0.0 - 1.0\ m$ (blue), $1.0 - 1.5\ m$ (green), $1.5 - 2.0\ m$ (yellow), and $2.0 - 2.5\ m$ (red)

Initiating an Operational Canadian Global Assimilation and Prediction Capability for the Coupled Atmosphere-Ocean-Ice System

*Hal Ritchie, Meteorological Research Division, EC, Dartmouth NS,
Doug Bancroft, Marine and Ice Services Division, EC, Ottawa ON
Greg Flato, Canadian Centre for Climate Modelling and Analysis, EC, Victoria BC
John Loder, Bedford Institute of Oceanography, DFO, Dartmouth NS
Normand Scantland, Directorate of Meteorology and Oceanography, DND, Ottawa ON
Keith Thompson, Department of Oceanography, Dalhousie University, Halifax NS
Dan Wright, Bedford Institute of Oceanography, DFO, Dartmouth NS

Environment Canada (EC), the Department of Fisheries and Oceans (DFO), and the Department of National Defence (DND) all need the products that can be provided by an operational global coupled atmosphere-ocean-ice data assimilation and prediction system. With the availability of global sea level and surface temperature observations from satellites and upper-ocean water mass properties from Argo floats, and the existence of moored arrays in the tropics, the development of a data-assimilative global ocean model for Canada is now feasible (as demonstrated by initiatives in France, Japan, and the UK and US). The natural next step is to develop a data-assimilative coupled atmosphere-ocean-ice system that will take full advantage of these new data sets.

The atmospheric GEM model currently used by EC in operational weather forecasting has state-of-the-art dynamics and assimilative methodologies, but it needs to be coupled to active ocean and ice models to improve forecasting skill in some areas. DFO has been a major contributor to the Argo float program but it has made only a limited investment in the development of the modeling capacity required to make full use of the resulting data. EC has recognized the potential for improved short-, medium- and long-range weather forecasts, and both DFO and DND recognize that they would benefit greatly from the availability of improved oceanic and meteorological information. Although the opportunity and the potential benefits are obvious, the development, maintenance and continued improvement of the required technology are major tasks that are beyond the present capacity of any one department. The success of such an initiative will require significant long-term contributions from all three departments as well as input from the academic research community.

Here we report on initial steps for Canada to implement and improve an operational assimilation and prediction capability for the coupled global atmosphere-ocean-ice system, referred to as the Canadian Operational Network of Coupled Environmental PredicTion Systems (CONCEPTS). The following paragraphs summarize the background developments and current status.

An Inter-agency Panel was formed in 2002 to make recommendations regarding the development of an operational coupled atmosphere-ocean-ice data assimilation and modelling capability. The Panel emphasized the following points in its report in January 2004:

1. A global system, with nested and coupled regional models dictated by scientific (e.g., tropical Pacific) and practical (northwest Atlantic, northeast Pacific) considerations, should be run

* *Corresponding author address*: Harold Ritchie, Environment Canada, 45 Alderney Drive, Dartmouth NS, Canada B2Y 2N6; E-mail: Harold.Ritchie@ ec.gc.ca

operationally at the Canadian Meteorological Centre (CMC) as an increment to the existing infrastructure.

2. New long-term funding and permanent positions should be established to support this new activity.
3. There is an excellent opportunity to benefit from, and contribute to the international Global Ocean Data Assimilation Experiment (GODAE) activity.
4. Suggested products to be developed in the short term (within three years) include: basin scale analyses of ocean temperature, salinity and currents for DFO and DND needs; global wave forecasts for operational DND needs; and a prototype coupled sea ice system.
5. Suggested products to be developed in the medium term (within five years) include: daily to seasonal forecasts of SST for atmospheric models, three-dimensional initial ocean fields for climate simulations, and global forecasts of large scale ocean temperature, salinity and currents, with nested basin-scale models, for operational DFO and DND needs.
6. Suggested products to be developed in the longer term (beyond five years) include an operational model-assimilation system for forecasting changes in the coupled global ocean-atmosphere-ice system and re-analyses of marine environmental conditions (e.g., hydrographic conditions, extreme currents at the shelf break, mean circulation patterns).
7. A two-track approach was recommended: a "fast track" based possibly on an imported system installed at CMC and extended to meet short-term goals and demonstrate the utility of Argo data; and a parallel slow track enhancing research and development for a system tailored to Canadian needs and generating Canadian capacity. It was subsequently decided to add a products activity as mentioned below.

The panel recommendations have been accepted by senior departmental managers, resulting in the development of the new CONCEPTS inter-agency initiative. In the past year agreement-in-principle has been reached with the Mercator group (France) to install a version of their ocean data assimilation and prediction system at CMC, and collaborate in a number of core research projects directed towards improved capabilities for atmosphere-ocean-ice prediction at various scales. Initial resources have been put in place for the establishment of three major inter-related activities: 1) an operational activity based on coupling the Canadian atmospheric GEM model with the Mercator system; 2) a research and development (R&D) activity consisting of government and academic research networks to develop and maintain a system tailored to Canadian needs in the longer term; and 3) a products activity to identify, develop and disseminate relevant products and outputs. The operational activity is being built upon existing EC infrastructure and centres on the following core projects: 1) core CMC systems installation, coupling and support; 2) basin-to-global ocean reanalyses for prediction and validation studies; 3) demonstration of regional ocean prediction capability and applications; 4) sea ice modelling and data assimilation; 5) improved ocean data assimilation capabilities; and 6) physical-biological ocean modelling. The R&D activity will be enhanced through a new research network on "Prediction and Predictability of the Global Atmosphere-Ocean System from Days to Decades" funded by the Canadian Foundation for Climate and Atmospheric Sciences.

Effects of horizontal resolution and sea surface cooling on simulations of tropical cyclones in case of Typhoon Namtheun (2004) by a coupled MRI tropical cyclone-ocean model.

Akiyoshi Wada and Akihiko Murata

Meteorological Research Institute, Tsukuba, Ibaraki, 305-0052, Japan
E-mail:awada@mri-jma.go.jp

1. Outline of numerical simulations

Numerical experiments were performed in case of Typhoon Namtheun (2004) by the coupled meteorological Research Institute (MRI) interactive multiply-nested movable mesh tropical cyclone-mixed layer slab ocean model (CTCM) to investigate the dependency of tropical cyclone (TC) intensity on the grid-spacing in the horizontal resolution in a coupled TC-ocean system.

Figure 1 illustrates the computational domain in the outer nest of CTCM with a horizontal grid-spacing of 6 km. The domain in the inner nest with a horizontal grid-spacing of 2 km is reallocated to involve the TC. The initial time of integration was at 0000 UTC 29 July 2004. The detail of experimental design was almost the same as that used in Wada and Mashiko (2006). However, cumulus parameterization of Grell (1993) and modified version of Deardorff (1983) entrainment parameterization are installed to the CTCM.

The numerical experiments by using the CTCM were conducted with a horizontal grid-spacing of 6 km alone and with horizontal grid-spaces of 2km and 6 km, respectively with/without the cumulus parameterization. Figure 2 denotes the procedures of numerical experiments. After the 30-hour integration in CTCM, numerical experiments with the two-nest version of CTCM were performed in cases with/without coupling with the ocean model. The numerical experiments with the cumulus parameterization were performed only with coupling with the ocean model.

Here, the numerical experiment in the one-nest without coupling the ocean model is called 'CNTL', that but with coupling the ocean model is called 'CPL'. In cases of the two-nest numerical experiments, '_2km' is added to each acronym. The numerical experiment by using the CTCM with the Grell's cumulus parameterization and modified Deardorff's entrainment parameterization is expressed as the acronym '_p'.

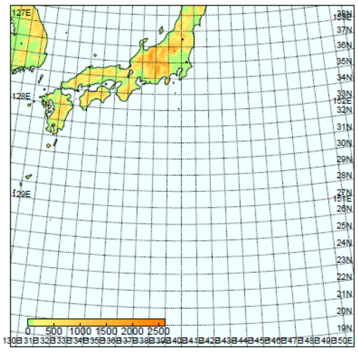

Fig.1 Computational domain in case of the numerical experiment with a horizontal grid-spacing of 6 km.

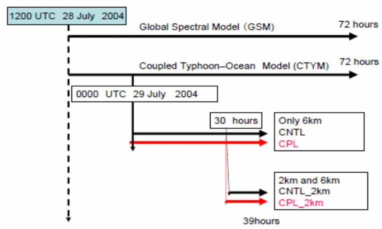

Fig.2 Procedures of numerical experiments

2. Results

2.1 Tropical cyclone intensity prediction

Predicted central pressures in CTCM are depicted in Fig. 3 every numerical experiments. The impact of local sea surface cooling (SSC) of TC intensity was initiated to appear around 21-hour integration. After 30-hour integration, the difference of central pressures between CNTL and CPL was larger than 5 hPa. After 30-hour integration, the difference of the central pressures became larger, which reached its peak of about 13hPa. In CNTL, rapid TC intensification occurred from 35-hour to 38-hour integration, while rapid TC intensification suppressed in CPL.

In CNTL_2km and CPL_2km, central pressures tended to be deeper than those in CNTL and CPL. The over-development suggests that finer horizontal resolutions enable TCs to further develop and intensify in CTCM. The peak of difference of central pressures between CNTL_2km and CPL_2km was about 9hPa, which was smaller than that between CNTL and CPL. The result of numerical experiment by CTCM in CPL_2km_p indicates that the prediction of the tendency of TC intensity is improved compared to the result in CPL_2km. This suggests that local SSC plays an important role in predicting realistic TC intensity. However, the role of cumulus parameterization in TC intensity has become an issue for further investigation.

2.2 Impact of horizontal resolution on local sea surface cooling and 1-hour precipitation

Figure 4 illustrates horizontal distribution of sea surface temperature (SST) and surface pressure at

36-hour integration in CNTL_2km (Fig. 4a), CPL_2km (Fig. 4b) and CPL_2km_p (Fig. 4c). Local SSC was significant around 137ºE, 32ºN where it was on the rightward of the moving direction of the TC. The amplitudes of SSC were the largest in CPL_2km_p.

Figure 5 illustrates horizontal distribution of 1-hour precipitation and surface pressure at 36-hour integration in CNTL_2km (Fig. 5a), CPL_2km (Fig. 5b), and CPL_2km_p (Fig. 5c). Outer spiral rainbands were simulated in CNTL_2km and CPL_2km, while those were not found in CPL_2km_p. Magnitude of 1-hour rainfall in Kii peninsula increased in all experiments, which was consistent with the observations (Wada, 2006). In contrast, broadly salient precipitations were found east of the TC vortex where it was behind the running direction in CPL_2km_p. The asymmetry of 1-hour precipitation may be related to the magnitude of local SSC. Moreover, the role of cumulus parameterization in asymmetry of 1-hour precipitation may be significant. These factors have now become an issue for further investigation.

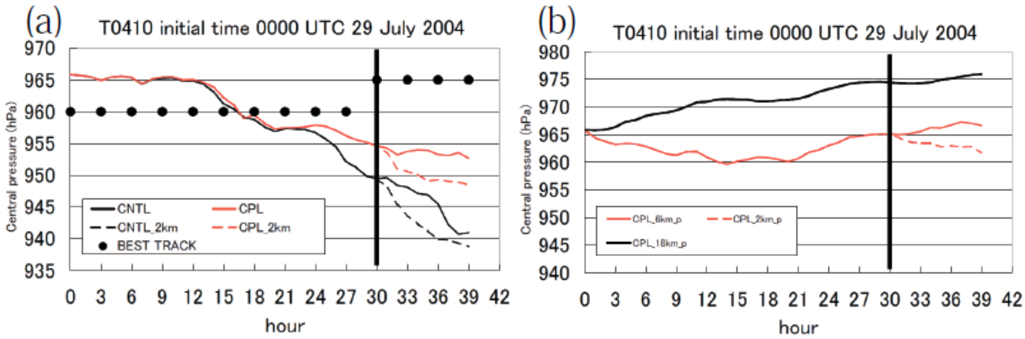

Fig. 3 Evolutions of central pressures (a) in CNTL, CPL, CNTL_2km, CPL_2km, and best track data, (b) in CPL and CPL_2km with the cumulus parameterization and modified Deardorff's entrainment parameterization.

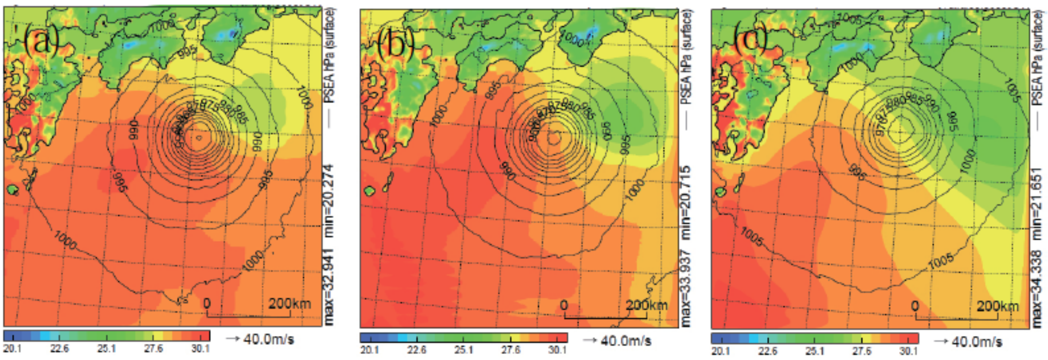
Fig. 4 Horizontal distribution of SST and surface pressure at 36-hour integration, (a) in CNTL_2km, (b) in CPL_2km, and (c) in CPL_2km with Grell's cumulus parameterization and modified Deardorff's entrainment parameterization.

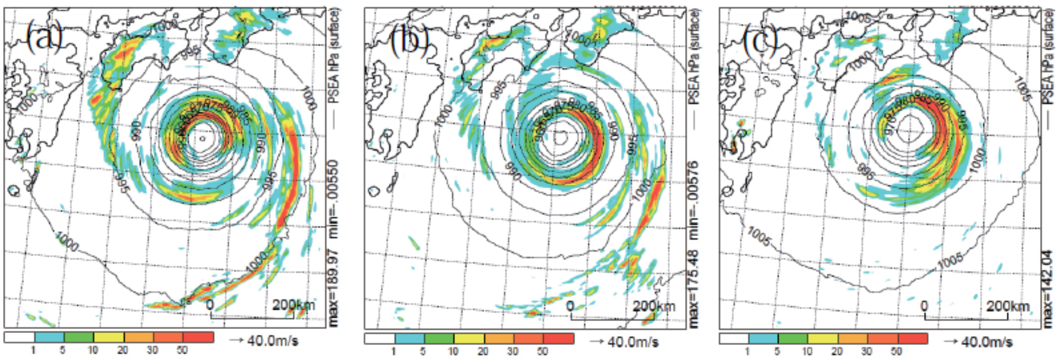
Fig. 5. Horizontal distribution of 1-hour precipitation and surface pressure at 36-hour integration, (a) in CNTL_2km, (b) in CPL_2km, and (c) in CPL_2km with Grell's cumulus parameterization and modified Deardorff's entrainment parameterization.

Acknowledgement

The authors are greatly appreciated to Mr. S. Ohmori and Mr. A. Shimpo for providing computational source codes of cumulus parameterization of Grell (1993).

References

Deardorff, J. W. (1983): A multi-limit mixed-layer entrainment formulation. *J. Phys. Oceanogr.*, **13**, 988-1002.

Grell, G. A. (1993): Prognostic evaluation of assumptions used by cumulus parameterizations. *Mon. Wea. Rev.*, **121**, 764-787.

Wada, A., and W. Mashiko (2006): Introduction of a mixed layer ocean model into the MRI interactive multiply-nested movable mesh tropical cyclone model. WMO CAS/JSC WGNE Report. 09-11.

Wada, A. (2006): Numerical experiments of Typhoon Namtheun (T0410) using different artmosphere-ocean coupled model. WMO CAS/JSC WGNE Report. 09-13.